

# Full-LIG Wireless Batteryless Sensor for the Detection of Amines

Andrea Salvia  
University of Rome Tor Vergata  
Rome, Italy  
a.salvia97@gmail.com

Alessio Mostaccio  
University of Rome Tor Vergata  
Rome, Italy  
alessio.mostaccio@uniroma2.it

Gianni Antonelli  
University of Rome Tor Vergata  
Rome, Italy  
g.antonelli@ing.uniroma2.it

Eugenio Martinelli  
University of Rome Tor Vergata  
Rome, Italy  
martinelli@ing.uniroma2.it

Gaetano Marrocco  
University of Rome Tor Vergata  
Rome, Italy  
gaetano.marrocco@uniroma2.it

**Abstract**—Food waste management at the global level requires new technologies for an item-level monitoring of the volatile molecules emitted by food inside the package. The use of conventional chemical sensors requiring complex electronics is prevented at the large scale by not affordable costs. A possible solution can come from the Laser-Induced Graphene (LIG) technology that permits to impress a complex circuit onto a polymeric substrate by means of laser engraving. We here propose the first zero-power wireless sensors on polyimide for amine detection, useful for hazard evaluation in case of consumption, where both the interdigitated sensor and the communication antenna are entirely made by LIG with non-uniform lasing parameters. The device is flexible, is capable of detecting less than 15% concentration of triethylamine and is readable up to 1.5m by resorting to the backscattering modulation framework of Radiofrequency Identification in the UHF band.

**Index Terms**—LIG, Graphene, Amine, Sensor, IDC, Antenna, RFID

## I. INTRODUCTION

Food waste management is a global issue stimulating serious environmental, economic, and social challenges. Almost one-third of the food produced per year (1.3 billion tonnes) is lost or discarded worldwide. The “food safety”, i.e. the “study of handling, preparation, and storage of food to prevent food-borne illness to the consumer” [1], takes therefore a remarkable importance.

Different volatile compounds, namely molecules whose presence above given concentrations is considered harmful for humans, can be targeted according to the food category. As a matter of fact, the oxygen inside the packaging is responsible for triggering the browning mechanism [2]. Ethylene is strongly correlated to fruit ripening [3]. The concentration of biogenic amines (BA), instead, is due to microbial metabolism [4], [5], and thus it is a direct indicator of the hazard in case of consumption. High levels of BA, indeed, cause food poisoning while a scarce concentration can lead to food intolerance [6]. The detection of the volatile analytes can be both qualitative and quantitative with the former lacking accuracy and the latter requiring expensive equipment.

There are several examples of sensors developed for the detection of gases and derivates, including BA; they generally employ conductive polymers or thin metal films [7], [8], but for the most, they involve both wired systems, not biocompatible materials and additional components which may contaminate the food.

Graphene is a valid candidate to boost the development of low-cost chemical sensors for integration into smart packaging thanks to its excellent electrical properties [9], biocompatibility [10] and the high surface area which make the material naturally sensitive to variable environmental conditions [11]–[13]. Unfortunately, graphene manufacturing process is time-consuming. In 2014 Lin *et al.*, introduced a lasing technique, denoted as LIG (Laser-Induced Graphene), to fabricate graphene starting from a polymeric precursor by means of a  $CO_2$  laser and without any additional material [14]. Sensors made of Laser-Induced Graphene have already been demonstrated for the detection of antibiotics (e.g. tetracycline [15] and chloramphenicol [11]), gases such as nitrogen monoxide [12] or biogenic amines as histamine [5]. They all required a wired system to collect readings.

This paper proposes, instead, the first wireless sensor ever for the amine measurement entirely made by LIG, namely both the sensing element (interdigital capacitor) and the antenna for data gathering are fabricated by lasing a same polyimide substrate. The communication link is established via backscattering modulation of the interrogating field resorting to the Radio-Frequency IDentification (RFID) platform at 868 MHz.

The paper is organized as follows. Section II introduces the layout and the design of the device, Section III describes the characterization of the communication and sensing performance by a preliminary prototype made through heterogeneous lasing settings.

## II. DEVICE LAYOUT AND OPTIMIZATION

The layout of the wireless sensor (Fig. 1) comprises a rectangular dipole, on a polyimide (PI) film 125  $\mu m$  thick ( $\epsilon_r = 3.5$ ,  $\tan(\delta) = 0.0026$  [16]) used as LIG precursor,

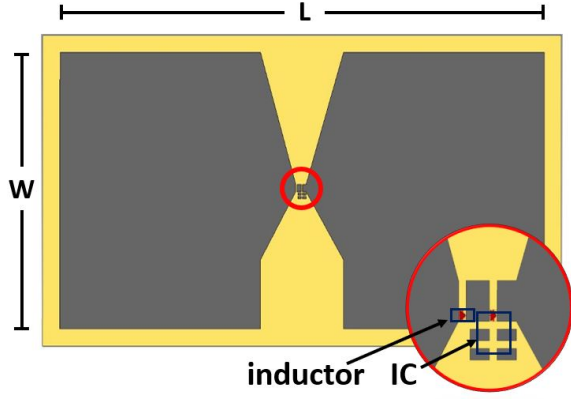


Fig. 1: Layout of LIG wireless sensor. Detail of the discrete components connection in the inset.

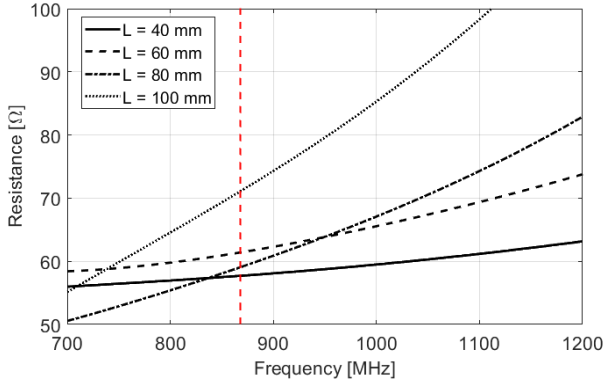


Fig. 2: Variation of antenna resistance w.r.t. to its length  $L$

whose central terminals are connected to an interdigital capacitor (IDC). The large width of the antenna is required to minimize the ohmic losses due to the modest conductivity of the graphene here assumed as  $\sigma = 12 \cdot 10^4 \text{ S/m}$  [17]. The IDC is coated by Poly(ethylene glycol) diacrylate (PEGDA) layer acting as the sensing part to the volatile analyte. The PEGDA layer captures the amine molecules which induce a morphological changes of the host layer. As a consequence, the dielectric permittivity of PEGDA shifts towards higher values.

Data will be collected and transmitted via backscattering modulation of an impinging field by the IC (Integrated Circuit) transponder EM Microelectronic em|aura-sense EM4152 [18] having internal impedance  $Z_{IC} = (24.7 - j284.3) \Omega$  at 868 MHz and activation power threshold  $P_{IC} = -18 \text{ dBm}$ . This IC is also provided with an analog part to sense a capacitance in the dynamic range  $0.15 \text{ pF} - 19.5 \text{ pF}$ . The size of the IC ( $1 \times 0.8 \text{ mm}$ ) is negligible with respect to that of the antenna, thus the flexibility of the device is not hindered by the presence of the discrete components.

#### A. Antenna Design

The impedance matching between antenna and IC is achieved in two steps by using a Finite Difference Time Domain (FDTD) solver (CST Studio 2023):

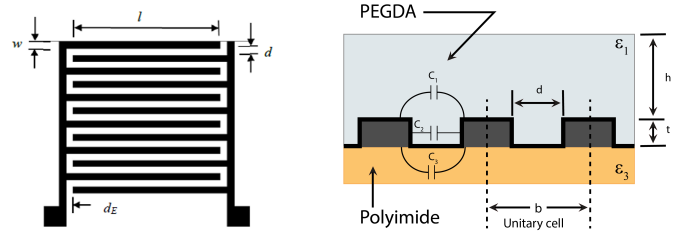


Fig. 3: Schematic of the interdigitated capacitor and contributions to total capacitance [19]

TABLE I: Geometrical parameters (in mm) of IDC with  $N = 12$  fingers

$l$	$w$	$d$	$b$	$d_E$
3	0.3	0.2	0.5	2

- the dipole width is fixed to  $W = 40 \text{ mm}$
- the real part of the IC is matched by acting on the dipole's length  $L$  (Fig. 2). The selected value is  $L = 70 \text{ mm}$
- the imaginary part is adjusted by a  $56 \text{ nH}$  inductor between the antenna and the IC.

The final antenna layout has an input impedance  $Z_A = (98.2 + j284.2) \Omega$  which grants a simulated power transfer coefficient  $\tau = 0.64$  and a realized gain  $\tilde{G} = -9.53 \text{ dBi}$ . By assuming an RFID reader with a circularly-polarized antenna emitting  $3.2 \text{ W EIRP}$  at 868 MHz (the maximum value allowed by the EU regulation), the device would be read up from a distance of  $1.6 \text{ m}$ .

#### B. Interdigitated capacitor design

According to [19], [20], the capacitance of the IDC can be expressed as

$$C_{\text{IDC}} = C_{uc}(n-1)l = (C_1 + C_2 + C_3)(n-1)l \quad (1)$$

where  $C_{uc}$  is the capacitance of the unitary cell,  $n$  the number of fingers and  $l$  the finger length (Fig. 3).  $C_{uc}$  is the sum of three contributes:  $C_1$  and  $C_3$  related through the fringe effect to the upper and lower substrate respectively and  $C_2$  (Fig. 3) which is instead proportional to the aspect ratio of the unitary cell.  $C_1$  and  $C_3$  are related (2) to the geometrical and material parameters as:

$$C_1 + C_3 = \epsilon_0 \left( \frac{\epsilon_1 + \epsilon_3}{2} \right) \frac{K \left[ \sqrt{1 - \left( \frac{d}{b} \right)^2} \right]}{K \left[ \frac{d}{b} \right]} \quad (2)$$

where  $\epsilon_1$  and  $\epsilon_3$  are the relative dielectric constant of the PEGDA and of the PI,  $d$  is the finger spacing,  $b = d + w$  the distance between the finger's centers, and  $K[x]$  the elliptic integral of the first kind.

The term  $C_2$  is the capacitance of a parallel plates capacitor:

$$C_2 = \epsilon_0 \epsilon_2 \frac{t}{d} \quad (3)$$

$\epsilon_0$  and  $\epsilon_2$  are the permittivity in free space and the permittivity of the material between the electrodes, i.e. PEGDA.

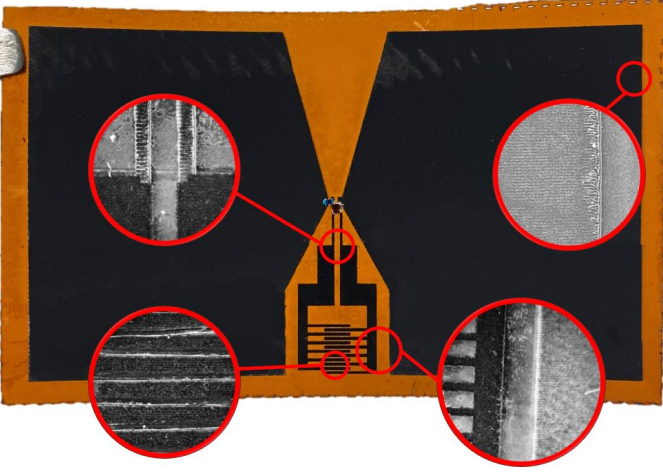


Fig. 4: Prototype of the full-LIG antenna plus sensor. Two kinds of lasing are visible: dark gray for the interdigitated capacitor, and light gray for the antenna.

The sizes of the IDC with 12 fingers are reported in Tab. I to achieve a simulated capacitance without PEGDA of 3 pF which fits the dynamic range of the RFID IC.

### III. PROTOTYPE AND MEASUREMENTS

#### A. Manufacturing

The device is finally manufactured by means of two different lasing settings through a Trotec Speedy 100 laser cutter starting from a polyimide sheet 125  $\mu\text{m}$  thick:

- the antenna, to improve the conductivity of LIG, was made by setting a laser power  $P = 9\text{ W}$ , a scan speed  $S_s = 10\text{ cm/s}$ , and a defocusing of 3 mm as in [17]. The resulting lased PI looks “light gray” (Fig. 4) and the measured sheet resistance was  $R_s = 12\ \Omega/\square$ . This manufacturing option grants better conductivity at the cost of lower precision due to the beam defocusing.
- the IDC was made by setting a laser power  $P = 5\text{ W}$  and a scan speed  $S_s = 5.4\text{ cm/s}$ , with no defocusing. The resulting engraved PI looks instead darker, and the measured sheet resistance was  $R_s = 85\ \Omega/\square$ .

During the engraving, PI was attached onto a 0.8 mm thick polymethylmethacrylate (PMMA) slab to minimize distortions of the substrate caused by the high local temperature increment.

The IC and the inductor were connected to the antenna by means of conductive epoxy (CW2400 by Chemtronics).

The sensing layer was achieved by drop casting [21] 15  $\mu\text{L}$  of PEGDA 575 and 1% of BAPO, a photoinitiator for the UV light-induced polymerization of acrylic resins [22]. The solution was deposited on the capacitor fingers through a Gilson pipette and then immediately exposed to UV light for approximately 10 seconds to cure the layer and prevent the spillage into unwanted areas. The final layout is reported in Fig. 4.

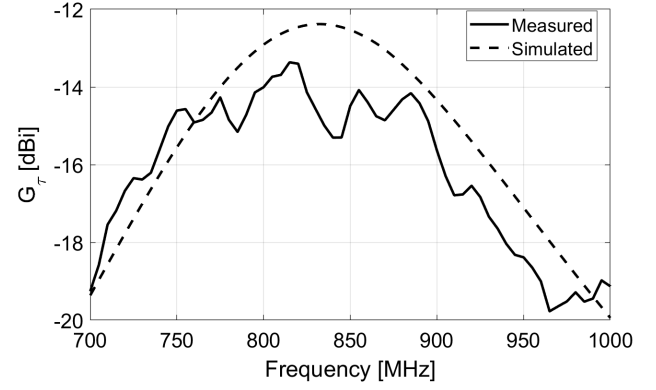


Fig. 5: Measured and simulated realized gain of the LIG transponder.

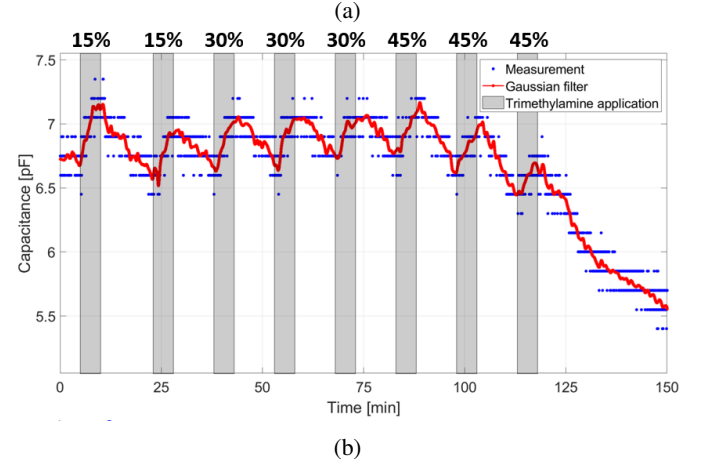
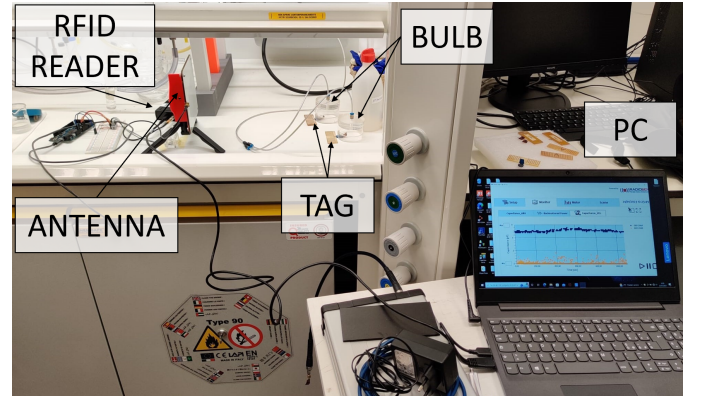


Fig. 6: (a) Measurement setup to evaluate the variation of fingers capacitance when exposed to amines. (b) Variation of IDC capacitance during the exposure; dots (in blue) are the measurement points, the solid curve (in red) is obtained by applying a Gaussian filter on the data to remove noise.

#### B. Communication characterization

The antenna performance was characterized by means of the UHF TagFormance<sup>®</sup> Station by Voyantic. Fig. 5 shows a good agreement with the measured and simulated realized

gain  $G_T$  over the frequency. The maximum estimated value is  $-13.5$  dB, granting a reading distance higher than 1 m. The difference between the two curves (2 dB at most), as well as the noise, is due to manufacturing imperfections.

#### C. Test of the sensor to amine exposure

The sensor was finally tested during the exposure to trimethylamine. The device was interrogated every 2 s by means of a custom software which controlled an RFID reader (ThingMagic® USB-Pro).

The device was placed under a PMMA bulb connected to a flowmeter and the amine/air aerosol was blown in the bulb for 5 min. Then, the sensor was cleaned with fresh air for 10 min. This procedure was repeated eight times by considering the following amine concentrations {15%, 15%, 30%, 30%, 30%, 45%, 45%, 45%} where 1% is approximately  $10^4$  ppm. Results are reported in Fig. 6b. Following the application of a Gaussian filter to remove noise, a clear response to the chemical stimuli (light gray bands) is visible. Instead, the sensor looks unable to identify the different levels of concentrations probably due to the partial saturation of the PEGDA coating. Perhaps a longer cleaning time would have been necessary between two consecutive cycles to release all the molecules captured.

#### IV. CONCLUSION

We have shown the first example (in our best knowledge) of an RFID transponder with sensing features which is fully made by lasing a piece of polyimide. Preliminary experiments demonstrated the potentiality to detect the presence of amines and transmit back this data up to 1.6 m.

Some critical issues are however still open, concerning a more appropriate design of the interdigitated capacitors and/or the selection of more convenient lasing parameters to avoid short circuits among thin traces in the micro-scale. Moreover, the sensitivity to the amine exposure must be accurately evaluated avoiding saturation to derive a calibration curve and assess the resolution of the sensor.

Overall, the idea of an all-in-one LIG device looks feasible and could have interesting applications to smart packaging capable to monitor the quality of food.

#### REFERENCES

- [1] L. Manning and J. M. Soon, "Food safety, food fraud, and food defense: a fast evolving literature," *Journal of food science*, vol. 81, no. 4, pp. R823–R834, 2016.
- [2] C. Gomes, M. E. Castell-Perez, E. Chimbombi, F. Barros, D. Sun, J. Liu, H.-J. Sue, P. Sherman, P. Dunne, and A. O. Wright, "Effect of oxygen-absorbing packaging on the shelf life of a liquid-based component of military operational rations," *Journal of food science*, vol. 74, no. 4, pp. E167–E176, 2009.
- [3] S. Yang and J. Oetiker, "The role of ethylene in fruit ripening," *Postharvest Physiology of Fruits* 398, pp. 167–178, 1994.
- [4] F. Galgano, F. Favati, M. Bonadio, V. Lorusso, and P. Romano, "Role of biogenic amines as index of freshness in beef meat packed with different biopolymeric materials," *Food Research International*, vol. 42, no. 8, pp. 1147–1152, 2009.
- [5] D. C. Vanegas, L. Patiño, C. Mendez, D. A. d. Oliveira, A. M. Torres, C. L. Gomes, and E. S. McLamore, "Laser scribed graphene biosensor for detection of biogenic amines in food samples using locally sourced materials," *Biosensors*, vol. 8, no. 2, p. 42, 2018.
- [6] S. L. Taylor and R. R. Eitenmiller, "Histamine food poisoning: toxicology and clinical aspects," *CRC Critical Reviews in Toxicology*, vol. 17, no. 2, pp. 91–128, 1986.
- [7] S. Karuppuswami, S. Mondal, D. Kumar, and P. Chahal, "Rfid coupled passive digital ammonia sensor for quality control of packaged food," *IEEE Sensors Journal*, vol. 20, no. 9, pp. 4679–4687, 2020.
- [8] H. Ahangari, S. Kurbanoglu, A. Ehsani, and B. Uslu, "Latest trends for biogenic amines detection in foods: Enzymatic biosensors and nanozymes applications," *Trends in Food Science & Technology*, vol. 112, pp. 75–87, 2021.
- [9] J. Phiri, P. Gane, and T. C. Maloney, "General overview of graphene: Production, properties and application in polymer composites," *Materials Science and Engineering: B*, vol. 215, pp. 9–28, 2017.
- [10] V. Vasilopoulos, M. Pitou, I. Fekas, R. Papi, A. Ouranidis, E. Pavlidou, P. Patsalas, and T. Choli-Papadopolou, "Graphene-wrapped copper nanoparticles: an antimicrobial and biocompatible nanomaterial with valuable properties for medical uses," *ACS omega*, vol. 5, no. 41, pp. 26 329–26 334, 2020.
- [11] A. R. Cardoso, A. C. Marques, L. Santos, A. F. Carvalho, F. M. Costa, R. Martins, M. G. F. Sales, and E. Fortunato, "Molecularly-imprinted chloramphenicol sensor with laser-induced graphene electrodes," *Biosensors and Bioelectronics*, vol. 124, pp. 167–175, 2019.
- [12] L. Yang, G. Zheng, Y. Cao, C. Meng, Y. Li, H. Ji, X. Chen, G. Niu, J. Yan, Y. Xue *et al.*, "Moisture-resistant, stretchable nox gas sensors based on laser-induced graphene for environmental monitoring and breath analysis," *Microsystems & nanoengineering*, vol. 8, no. 1, pp. 1–12, 2022.
- [13] M. G. Stanford, K. Yang, Y. Chyan, C. Kittrell, and J. M. Tour, "Laser-induced graphene for flexible and embeddable gas sensors," *ACS nano*, vol. 13, no. 3, pp. 3474–3482, 2019.
- [14] R. Ye, D. K. James, and J. M. Tour, "Laser-induced graphene: from discovery to translation," *Advanced Materials*, vol. 31, no. 1, p. 1803621, 2019.
- [15] B. D. Abera, I. Ortiz-Gómez, B. Shkodra, F. J. Romero, G. Cantarella, L. Petti, A. Salinas-Castillo, P. Lugli, and A. Rivadeneyra, "Laser-induced graphene electrodes modified with a molecularly imprinted polymer for detection of tetracycline in milk and meat," *Sensors*, vol. 22, no. 1, p. 269, 2021.
- [16] DuPont, "Kapton® fpc - datasheet," <https://www.dupont.com/content/dam/dupont/amer/us/en/products/ei-transformation/documents/K-15361-Kapton-FPC-DataSheet.pdf>, 02 2023.
- [17] A. Mostaccio, G. Antonelli, C. Occhiuzzi, E. Martinelli, and G. Marrocco, "Experimental characterization of laser induced graphene (lig) antennas for s-band wearable applications in 5g," in *2022 IEEE 12th International Conference on RFID Technology and Applications (RFID-TA)*. IEEE, 2022, pp. 51–54.
- [18] EM Microelectronic, "em|aura-sense em4152 rain rfid™ transponder ic with capacitive sensor interface - datasheet," <https://www.emmicroelectronic.com/sites/default/files/products/datasheets/4152-DS%20v4.2.pdf>, 02 2023.
- [19] D. Sinar and G. K. Knopf, "Printed graphene interdigitated capacitive sensors on flexible polyimide substrates," in *14th IEEE International Conference on Nanotechnology*. IEEE, 2014, pp. 538–542.
- [20] M. A. al Rumon and H. Shahariar, "Fabrication of interdigitated capacitor on fabric as tactile sensor," *Sensors International*, vol. 2, p. 100086, 2021.
- [21] H. Li, C. Guo, C. Liu, L. Ge, and F. Li, "Laser-induced graphene hybrid photoelectrode for enhanced photoelectrochemical detection of glucose," *Analyst*, vol. 145, no. 11, pp. 4041–4049, 2020.
- [22] C. T. Meereis, F. B. Leal, G. S. Lima, R. V. de Carvalho, E. Piva, and F. A. Ogliari, "Bapo as an alternative photoinitiator for the radical polymerization of dental resins," *Dental materials*, vol. 30, no. 9, pp. 945–953, 2014.